JOURNAL OF THE
ELECTRON DEVICES SOCIETY

Received 18 March 2022; accepted 31 March 2022. Date of publication 7 April 2022; date of current version 18 April 2022.
The review of this article was arranged by Editor C. C. McAndrew.

Digital Object Identifier 10.1109/JEDS.2022.3165534

AlGaN/GaN Schottky Barrier Diodes on Free-Standing GaN Substrates With a Si Doped Barrier Layer

TAOFEI PU[1,2], HSIANG-CHUN WANG[1,2], KUANG-PO HSUEH[3,4],
HSIEN-CHIN CHIU[3,4] (Senior Member, IEEE), AND XINKE LIU[5] (Member, IEEE)

1 College of Materials Science and Engineering, Shenzhen University–Hanshan Normal University Postdoctoral Workstation, Shenzhen University, Shenzhen 518060, China
2 Key Laboratory of Optoelectronic Devices and Systems of Ministry of Education and Guangdong Province, College of Physics and Optoelectronic Engineering, Shenzhen University, Shenzhen 518060, China
3 Department of Electronics Engineering, Chang Gung University, Taoyuan 33302, Taiwan
4 Department of Digital Multimedia Technology, Vanung University, Taoyuan 32061, Taiwan
5 College of Materials Science and Engineering, Shenzhen University, Shenzhen 518060, China

CORRESPONDING AUTHOR: X. LIU (e-mail: xkliu@szu.edu.cn)

This work was supported in part by the National Natural Science Foundation of China under Grant 61974144 and Grant 62004127; in part by the Key-Area Research and Development Program of Guangdong Province under Grant 2020B010174003; in part by the Guangdong Science Foundation for Distinguished Young Scholars under Grant 2022B1515020073; and in part by the Science and Technology Foundation of Shenzhen under Grant JSGG20191129114216474.

ABSTRACT This paper presented a AlGaN/GaN Schottky barrier diodes (SBDs) on free-standing GaN substrates with a Si doped barrier layer were fabricated for high power application. Compared with the conventional SBDs, the SBDs with doped barrier layer have the lower turn-on voltage (V_{ON}) and specific on resistance (R_{ON_SP}) because more free carriers are induced in two-dimensional electron gas (2DEG) channel. With Si doping concentration of 1×10^{20} cm^{-3} for AlGaN barrier layer, the SBDs demonstrate R_{ON_SP} of 0.12 mΩ·cm^2, V_{ON} of 0.41 V, breakdown voltage of 339 V, and power figure-of-merit ($PFOM$) of 957.6 MV/cm^2, which have a great potential for high-speed power device applications. Meanwhile, the SBDs with doped barrier have a faster reverse recovery time, and a better low-frequency noise (LFN) characteristics at low current density due to high carrier mobility and less generation-recombination (G-R) noise.

INDEX TERMS AlGaN/GaN, Schottky barrier diode, Si doped, AlGaN barrier layer.

I. INTRODUCTION

Recently, GaN-based devices have shown great potential for applications in high-speed power conversion systems due to their excellent physical properties, including wide band gap, high critical field for breakdown, and high electron mobility, compared with other commercial semiconductor materials [1]–[2]. GaN-based devices on Si or SiC substrate have attracted much attention due to their low cost and the superior scalability of wafer production [3]–[5]. However, the threading dislocation and defects between the grown GaN epitaxial layer and foreign substrate lead to nonlinearity output at high output power communication applications [6]. Thus, free-standing bulk GaN with low threading dislocation density has been used as a latticed matched substrate for AlGaN/GaN heterostructure devices [6], [7].

AlGaN/GaN heterostructure devices are widely utilized in radio frequency (RF) and power application systems due to high concentration and high mobility of two-dimensional electron gas (2DEG). They can provide high switching speed, low reverse recovery loss, and the high reverse breakdown voltage (V_{BR}). AlGaN/GaN heterostructure diodes are required to have a low turn-on voltage (V_{ON}) and specific on resistance (R_{ON_SP}) without sacrificing the reverse characteristics to minimize power loss during operation of power circuits and systems [8], [9]. Some technologies have been reported to improve the performance of diodes. In particular, the recessed anode structure has been investigated widely because it can lower the V_{ON} and improve the V_{BR} values of Schottky barrier diodes (SBDs) owing to the thinner barrier layer between Schottky anode metal and

GaN channel layer [10]–[12]. However, the lattice damage induced by inductively coupled plasma (ICP) dry etching and the after treatment of etched surface are inevitable during the fabrication of recessed anode structure, thereby increasing the complexity of fabrication and the difficulty of mass production [13]. Anode metals with low work function (e.g., TiN) are utilized to replace the common Ni anode for achieving a low V_{ON}, but an issue of high reverse leakage current. In addition to V_{ON}, the resistance of the device working at low power conditions, which is limited by 2DEG concentration and mobility, is extremely important owing to the 2DEG-dependent conductivity for AlGaN/GaN diode. Thus, the extra free charge, which is from n-type doping, is needed to reduce the resistance of GaN-based devices.

In this study, we proposed an alternative method to reduce the V_{ON} and achieve an ultralow R_{ON_SP} during the fabrication of conventional Ni anode with AlGaN/GaN SBD under low power conditions for minimizing power loss. The AlGaN/GaN SBD with Si modulation doped barrier, which was used in modulation doped field-effect transistor (MODFET) previously, was fabricated. The V_{ON} was reduced by using a Si doped AlGaN barrier to obtain high electron concentration that can increase the rate of electron tunneling and hopping. The doped AlGaN layer was sandwiched by two undoped AlGaN barrier layers to keep away from the 2DEG channel for alleviating the effect of dopant on 2DGE mobility due to impurity scattering in channel [15]. The Si doped AlGaN barrier significantly reduced the device resistance, thereby reducing power loss in practice. The free standing GaN substrate was also adopted to achieve a great lattice quality.

The Current-voltage (*I*-*V*) characteristics at forward and reverse directions were discussed in detail. The SBD with Si doped AlGaN barrier layer demonstrated lower V_{ON} and R_{ON_SP}, which is a tradeoff with reverse leakage current and V_{BR} performance. The reverse recovery characteristic and low-frequency noise (LFN) of the AlGaN/GaN SBDs were measured for further analysis.

II. EXPERIMENT

In Fig. 1a, the epitaxial structure of AlGaN/GaN SBD was grown on a 2-inch insulated Fe-doped free-standing GaN substrate (350 μm) with (0001) orientation by metalorganic chemical vapor deposition (MOCVD). The vertical structure of the reference wafer consists of a thin AlN nucleation layer, a Fe-doped GaN buffer layer (5 μm), and $Al_{0.25}Ga_{0.75}N$/GaN (18/300 nm) heterostructure from bottom to top. A 1.5-nm-thick GaN was grown as the cap layer. The AlGaN barrier layer of 18 nm was divided into three parts of 9, 8, and 1 nm from top to bottom. Only the middle AlGaN layer of 8 nm was doped with various Si doping concentrations, which were undoped (labeled as structure L), 1×10^{19} cm^{-3} (labeled as structure M), and 1×10^{20} cm^{-3} (labeled as structure H), respectively. The other parts of AlGaN layer were undoped. This design was investigated to achieve lower turn-on voltage and higher switching speed.

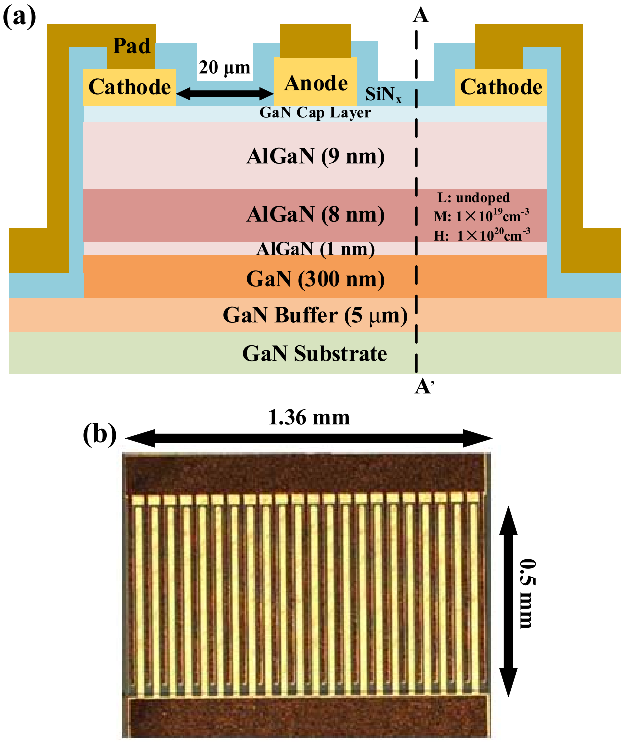

FIGURE 1. **(a) A schematic cross-section view of AlGaN/GaN SBDs with varied Si doping concentration in the AlGaN barrier layer. (b) A top view photograph of SBD in this study.**

The fabrication of SBDs was based on the standard photolithography and lift-off technology. The fabrication process was started with device isolation. After wafer cleaning by SPM and organic solution, mesa dry etching was conducted by combining BCl_3, Cl_2, and Ar gases, using a photoresistor as mark. Then, Ti/Al/Ni/Au (30/125/50/200 nm) as cathode ohmic stack was deposited by electron beam evaporation. Ohmic contact was obtained by rapid thermal annealing at 850 °C for 30 sec in N_2 atmosphere. The contact resistance is 2.12×10^{-5} cm^2 (structure L) and 1.3×10^{-6} cm^2 (structure M and H), respectively, which is due to the high 2DEG density induced by Si doping concentrations. A finger-type anode with a width of 500 μm and a length of 20 μm was formed by evaporating a Ni/Au (25/100 nm) stack and subsequent lift-off process. Finally, a thick SiN_x layer was deposited as a passivation layer, with the pad formed by a Ti/Au (25 nm/1000 nm) metal stack. A top view photograph of the SBDs is shown in Fig. 1b. The distance of anode-to-cathode (L_{AC}) was 20 μm. The active region size of the device was 680,000 μm^2 (1360 μm × 500 μm).

III. RESULTS AND DISCUSSION

Through TCAD simulation, the conduction band diagrams along the cutline from A to A' in Fig. 1a of AlGaN/GaN SBDs in structure L, M, and H are shown in Fig. 2a. Compared with structure L, an obvious conduction band bending can be observed in the doped AlGaN barrier layer. For structure H, a portion of conduction band is below the

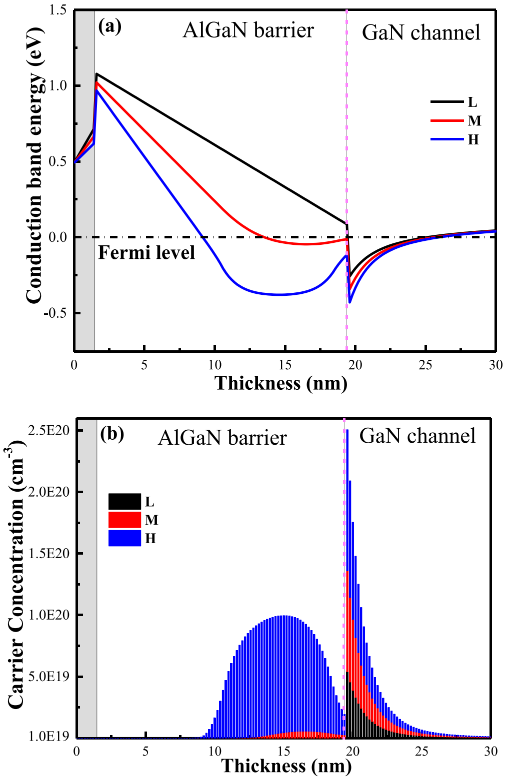

FIGURE 2. **(a) Conduction band diagrams at anode voltage of 0 V, and (b) carrier concentration distribution for structure L, M and H, respectively.**

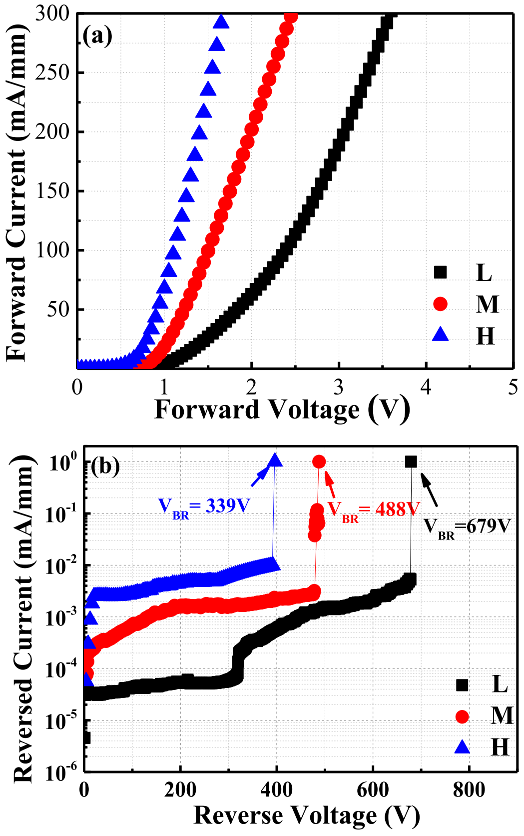

FIGURE 3. **(a) Forward current-voltage (*I–V*) characteristics, and (b) reversed current-voltage (*I–V*) characteristics (semi-log scale) for structure L, M and H, respectively.**

Fermi level. The Si dopant and donor-like defects/impurities in AlGaN/GaN heterostructure are regarded as n-type doping, and the resulted band bending for AlGaN barrier layer induces more carrier in the channel, easily resulting in the band to band tunneling.

Nevertheless, the conduction band of AlGaN/GaN interface shows a slight falling of structure M and H, resulting in higher carrier concentration of 1.5×10^{20} and 2.5×10^{20} cm^{-3}, respectively, compared with structure L of 5.4×10^{19} cm^{-3}. Consequently, the doped barrier layer induces a lower sheet resistance than that of undoped one, and the lowest sheet resistance of 330 Ω/square is found in structure H at 300 K. This finding indicates that the 2DEG concentration slight increases due to the effect of doped AlGaN barrier layer. The hall mobility was measured. The structure M and H have a lower carrier mobility due to the impurity scatter caused by dopant. Among them, structure H demonstrates the lowest carrier mobility of 840 cm^{2}V^{-1}s^{-1} at 300 K.

The DC characteristics of the three structures were measured by using an Agilent B1505A measurement system with substrate grounding. The curves of forward current-voltage (*I–V*) characteristics are demonstrated in Fig. 3a. The V_{ON} values of structures L, M, and H at the forward current of 1 mA/mm were 0.83, 0.68, and 0.41 V, respectively. The R_{ON_SP} values of L, M. and H defined at the voltage of 1.5 V were 1.12, 0.30, and 0.12 mΩ·cm^2, indicating a low power loss in practice.

The reversed breakdown characteristics of the SBDs at 300 K are presented in Fig. 3b, which is the median among the measured devices. V_{BR} is defined as the reverse current density reaching 1 mA/mm. The reverse leakage current of the structure L below the −300 V bias was lower by more than an order of magnitude than that of structures M and H. The soft V_{BR} value of structure L was about 320 V, which is no existent for structure M and H due to high reverse leakage current. The hard V_{BR} values of structures L, M, and H were 679, 488, and 339 V, respectively. This result reveals that increasing doping concentrations in the barrier layer slightly raises the reverse leakage current and decreases the V_{BR} value because the free carriers transiting from the doped barrier layer to the 2DEG channel are out of limit. The extracted parameters of structure L, M, and H and that of other studies at 300K are summarized in Table 1. The power figure-of-merit ($PFOM = V_{BR}^2/R_{ON\_SP}$) values of structure L, M, and H were calculated as 411.6, 793.8, and 957.6 MW/cm^2, respectively. Among these structures, structure H shows the highest *PFOM* due to the ultralow R_{ON_SP} induced by more free carriers in the channel layer. Although our device is not the best in terms of various single

TABLE 1. DC characteristics of structure L, M AND H AT 300K.

Structure	V_{ON} @1mA/mm V	I_F@1.5V mA/mm	$R_{ON,SP}$ mΩ·cm²	V_{BR} V	*PFOM* MW/cm²
Structure L (Undoped)	0.83	26.8	1.12	679	411.6
Structure M (1×10^{19} cm^{-3})	0.68	99.4	0.30	488	793.8
Structure H (1×10^{20} cm^{-3})	0.41	234.8	0.12	339	957.6
[8]	1.0	--	--	1500	666.7
[9]	0.7	85	5.12	1900	727
[10]	0.73	--	3.8	2070	1127
[16]	0.1	--	4.26	606	86.2

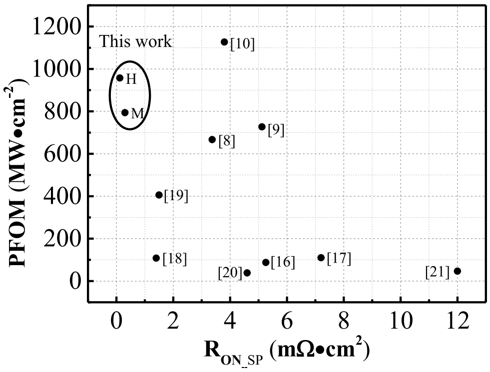

FIGURE 4. Benchmark plot of R_{ON_SP} versus *PFOM* for lateral GaN-based SBDs.

parameters, its comprehensive performance is outstanding and has relatively simple fabrication process.

Fig. 4 shows the benchmarks of the specific ON-resistance versus *PFOM* for various lateral AlGaN/GaN SBDs. Owing to the ultralow R_{ON_SP} value, the AlGaN/GaN SBDs with doped barrier layer demonstrate relatively high *PFOM* compared with other SBDs, which is promising for power applications.

The Schottky barrier height (SBH) and ideality factors (n) are extracted from Fig. 3a, which can be analyzed on the basis of thermionic emission-diffusion theory, to further investigating the current characteristics of structure M and H. The I-V characteristic of SBDs at forward-bias is expressed as the following relationship [22]–[23]:

$$J = A^{**}T^2 \exp\left(-\frac{q\Phi_b}{kT}\right)\left[\exp\left(\frac{qV}{nkT}\right) - 1\right] \qquad (1)$$

where A^{**} is the effective Richardson constant, which is 26.04 Acm^{-2}K^{-2} for n-GaN, T is the absolute temperature, q is the electron charge, ϕ_b is the zero-bias apparent SBH, k is the Boltzmann constant, V is the forward-bias voltage, n is the ideality factor, and J is the current density. From equation (1), the extracted SBHs and ideality factors were 0.868, 0.763, 0.6 eV and 1.64, 2.46, 3.03 for structure L, M, and H, respectively. The SBH of doped SBDs demonstrates an inversely proportional relationship with increased doping concentrations of inner barrier layer, which depends strongly on the band discontinuities and anode contact defects. The energy band plots in Fig. 2a reveal that the conduction band of anode/AlGaN and AlGaN/GaN interface slightly decreases with respect to the conventional SBD, which is due to the doped inner AlGaN barrier layer. On the other hand, the high value of ideality factors structure M and H indicates that thermionic emission-diffusion theory and other mechanisms contribute to the diode current. Therefore, the high concentration of the inner AlGaN barrier layer influences the conductive mechanism although it's not directly contacting with GaN channel layer, thereby enhancing the carrier tunneling effect through the anode/AlGaN and AlGaN/GaN interface. Hence, the SBH of structure M and H is dominated by band discontinuities, anode contact defects and dopant influence, simultaneously by combining with the Schottky contact interface of anode/undoped AlGaN. When the doped SBD is under reverse bias, the doped inner barrier layer cannot be depleted entirely, resulting in a high leakage current and a relatively low breakdown voltage.

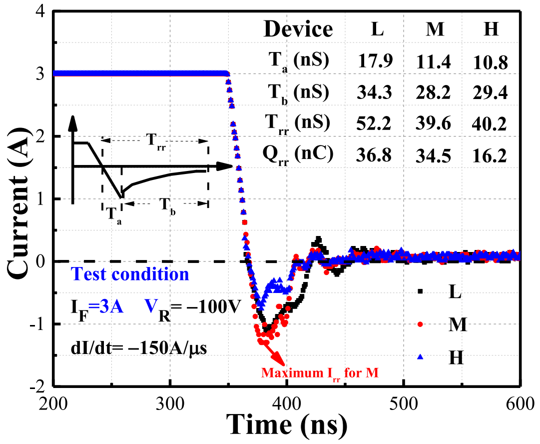

FIGURE 5. Reverse recovery characteristics for structure L, M and H, respectively.

Fig. 5 illustrates the reverse recovery characteristics of structures L, M, and H measured with a Poworld Electronic PQR 600 tester system. The switched conditions were set up at the forward current of IF = 3 A, followed by switching to the reverse bias of −100 V with dI/dt of 150 A/μs at room temperature. Reverse recovery time (T_{rr}) is the sum of storage time (T_a) and reverse current delay time (T_b). T_b is defined at the time of the diode current recovering to 10% of I_{rr}, in which I_{rr} is the maximum reverse recovery current [24]. Reverse recovery charge (Q_{rr}) is the charge accumulated within a diode rectifier that has experienced a forward current. When switching to reverse bias, this charge is released as a reverse current for an amount of time known as T_{rr}. T_{rr} values of 52.2, 39.6 and 40.2 ns were extracted for structures L, M, and H, respectively. Structure M and H have faster recovery characteristics than L, which is attributed to

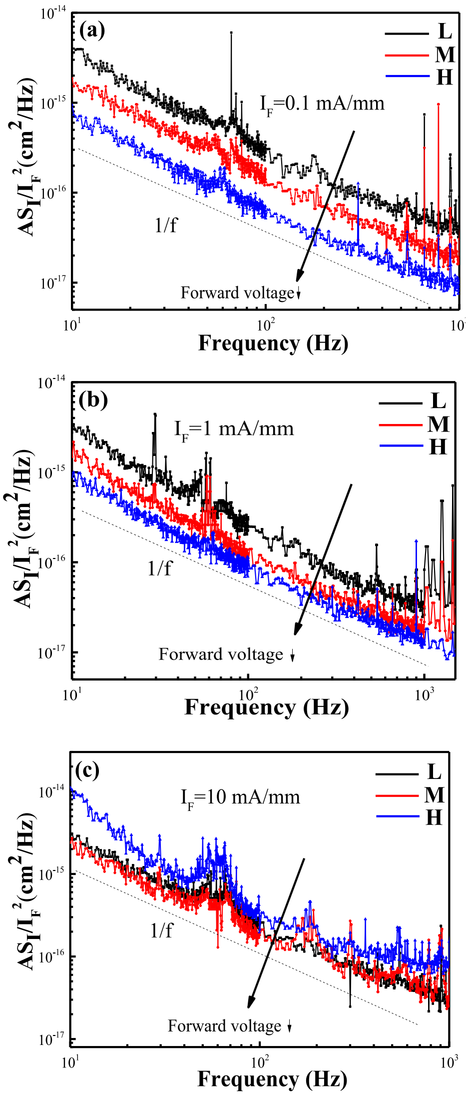

FIGURE 6. **The noise spectral versus frequency for structure L, M and H with current density of (a) 0.1, (b) 1, and (c) 10 mA/mm at 300 K.**

the strong tunneling effect. Structure L and M have sharp reverse recovery characteristics, and structure H shows a soft reverse recovery waveform. Therefore, a structure M combining with a lower value of T_b, exhibits a slightly faster T_{rr} than that of structure H. However, the low ability of storing charge induced by high doping concentration results in the lowest reverse recovery charge Q_{rr} of 16.2 nC for structure H. Structure H has the most excellent reverse recovery characteristics by comprehensive analyzing the parameters of reverse recovery curves.

The measurement of LFN spectra as a crucial factor in microwave and high-power system applications was performed by utilizing the fluctuation of forward current caused by the charging or discharging of defects in the anode area. This process was conducted to further analyze the trapping phenomenon of AlGaN barrier layer with varied doping concentration. The frequency ranging from 10 to 1000 Hz and the current density varying from 0.1, 1 to 10 mA/mm around the turn-on voltage of SBDs, for structure L, M, and H were set up. Fig. 6 shows the measured LFN spectra of SBDs depending on frequency with different current densities at T = 300 K. The curves show that the LFN of doped SBDs is lower at low current of 0.1 and 1 mA/mm owing to the bandgap bending and widened 2DEG channel. However, the doping SBDs have high noise at a higher current density of 10 mA/mm. This condition is due to the trapping effect lower than the carrier mobility in the 2DEG channel and more generation-recombination (G-R) noise caused by high doping concentration.

IV. CONCLUSION

AlGaN/GaN SBDs with different Si doped AlGaN barrier layer, in which the doped layer was sandwiched by two undoped AlGaN barrier layer, were fabricated on free-standing GaN substrates to further improve V_{ON}, and R_{ON_SP}. The SBDs with doped AlGaN barrier layer had lower V_{ON} and R_{ON_SP} than the undoped SBDs because more numerous free carriers were induced in 2DEG channel. The SBDs with Si doping concentration of 1×10^{20} cm^{-3} (structure H) had R_{ON_SP} of 0.12 mΩ·cm^2, V_{ON} of 0.41 V, breakdown voltage of 339 V, the highest PFOM of 957.6 MV/cm^2 and the excellent reverse recovery characteristics as well which is great potential for high-speed power device applications. And the LFN characteristics demonstrated that low noise was confirmed for SBDs with doped barrier layer at low current density, but high noise at high level of current density (10 mA/mm) due to reduced carrier mobility and more G-R noise generated.

ACKNOWLEDGMENT

The authors would like to thank the professional noise spectral measurements and valuable discussions from the Department of Electronics Engineering, Chang Gung University, for this work.

REFERENCES

[1] S. Lenci *et al.*, “Au-free AlGaN/GaN power diode on 8-in Si substrate with gated edge termination,” *IEEE Electron Device Lett.*, vol. 34, no. 8, pp. 1035–1037, Aug. 2013, doi: 10.1109/LED.2013.2267933.

[2] S. J. Pearton and F. Ren, “GaN electronics,” *Adv. Mater.*, vol. 12, no. 21, pp. 1571–1580, Nov. 2000. [Online]. Available: https://onlinelibrary.wiley.com/doi/abs/10.1002/1521-4095(200011)12:21%3C1571::AID-ADMA1571%3E3.0.CO;2-T

[3] M. Ishida, T. Ueda, T. Tanaka, and D. Ueda, “GaN on Si technologies for power switching devices,” *IEEE Trans. Electron Devices*, vol. 60, no. 10, pp. 3053–3059, Oct. 2013, doi: 10.1109/TED.2013.2268577.

[4] J. Cheng *et al.*, “Growth of high quality and uniformity AlGaN/GaN heterostructures on Si substrates using a single AlGaN layer with low AL composition,” *Sci. Rep.*, vol. 6, Mar. 2016, Art. no. 23020, doi: 10.1038/srep23020.

[5] S. Arulkumaran *et al.*, “High-frequency microwave noise characteristics of InAlN/GaN high-electron-mobility transistors on Si (111) substrate,” *IEEE Electron Device Lett.*, vol. 35, no. 10, pp. 992–994, Oct. 2014, doi: 10.1109/LED.2014.2343455.

[6] X. Liu *et al.*, “Analysis of the back-barrier effect in AlGaN/GaN high electron mobility transistor on free-standing GaN substrates,” *J. Alloys Compd.*, vol. 814, Jan. 2020, Art. no. 152293. [Online]. Available: https://doi.org/10.1016/j.jallcom.2019.152293

[7] X. Liu *et al.*, “AlGaN/GaN high electron mobility transistors with a low sub-threshold swing on free-standing GaN wafer,” *AIP Adv.*, vol. 7, no. 9, Sep. 2017, Art. no. 095305, doi: 10.1063/1.4999810.

[8] Y.-W. Lian, Y.-S. Lin, J.-M. Yang, C.-H. Cheng, and S. S. H. Hsu, “AlGaN/GaN schottky barrier diodes on silicon substrates with selective Si diffusion for low onset voltage and high reverse blocking,” *IEEE Electron Device Lett.*, vol. 34, no. 8, pp. 981–983, Aug. 2013, doi: 10.1109/LED.2013.2269475.

[9] M. Zhu *et al.*, “1.9-kV AlGaN/GaN lateral schottky barrier diodes on silicon,” *IEEE Electron Device Lett.*, vol. 36, no. 4, pp. 375–377, Apr. 2015, doi: 10.1109/LED.2015.2404309.

[10] C.-W. Tsou, K.-P. Wei, Y.-W. Lian, and S. S. H. Hsu, “2.07-kV AlGaN/GaN schottky barrier diodes on silicon with high Baliga’s figure-of-merit,” *IEEE Trans. Electron Devices.*, vol. 37, no. 1, pp. 70–73, Nov. 2016, doi: 10.1109/LED.2015.2499267.

[11] Y. Yao *et al.*, “Current transport mechanism of AlGaN/GaN Schottky barrier diode with fully recessed Schottky anode,” *Jpn. J. Appl. Phys.*, vol. 54, no. 1, Dec. 2015, Art. no. 011001. [Online]. Available: http://doi.org/10.7567/JJAP.54.011001

[12] J. Hu *et al.*, “Statistical analysis of the impact of anode recess on the electrical characteristics of AlGaN/GaN schottky diodes with gated edge termination,” *IEEE Trans. Electron Devices*, vol. 63, no. 9, pp. 3451–3458, Sep. 2016, doi: 10.1109/TED.2016.2587103.

[13] W. Ha *et al.*, “Analysis of the reverse leakage current in AlGaN/GaN Schottky barrier diodes treated with fluorine plasma,” *Appl. Phys. Lett.*, vol. 100, Mar. 2012, Art. no. 132104. [Online]. Available: http://doi.org/10.1063/1.3697684

[14] L. Li, J. Chen, X. Gu, X. Li, T. Pu, and J.-P. Ao, “Temperature sensor using thermally stable TiN anode GaN Schottky barrier diode for high power device application,” *Superlattices Microstruct.*, vol. 123, pp. 274–279, Nov. 2018. [Online]. Available: http://doi.org/10.1016/j.spmi.2018.09.007

[15] S. Heikman, S. Keller, D. S. Green, S. P. DenBaars, and U. K. Mishra, “High conductivity modulation doped AlGaN/GaN multiple channel heterostructures,” *J. Appl. Phys.*, vol. 94, no. 8, pp. 5321–5325, Sep. 2003. [Online]. Available: http://doi.org/10.1063/1.1610244

[16] K.-P. Hsueh *et al.*, “Effect of the AlGaN/GaN schottky barrier diodes combined with a dual anode metal and a p-GaN layer on reverse breakdown and turn-on voltage,” *Mater. Sci. Semicond. Process.*, vol. 90, pp. 107–111, Feb. 2019. [Online]. Available: http://doi.org/10.1016/j.mssp.2018.10.013

[17] T.-F. Chang *et al.*, “Low turn-on voltage dual metal AlGaN/GaN Schottky barrier diode,” *Solid-State Electron.*, vol. 105, pp. 12–15, Mar. 2015. [Online]. Available: http://doi.org/10.1016/j.sse.2014.11.024

[18] H.J. Che *et al.*, “Robust reproducible large-area molecular rectifier junctions,” *Appl. Phys. Lett.*, vol. 92, no. 25, Jun. 2008, Art. no. 253503. [Online]. Available: http://doi.org/10.1063/1.2940592

[19] E. B. Treidel, O. Hilt, A. Wentzel, J. Würfl, and G. Tränkle, “Fast GaN based Schottky diodes on Si (111) substrate with low onset voltage and strong reverse blocking,” *Physica Status Solidi C*, vol. 10, no. 5, pp. 849–852, Jan. 2013. [Online]. Available: http://doi.org/10.1002/pssc.201200569

[20] W. Lim *et al.*, “Temperature dependence of current-voltage characteristics of Ni–AlGaN/GaN Schottky diodes,” *Appl. Phys. Lett.*, vol. 97, no. 24, Dec. 2010, Art. no. 242103. [Online]. Available: http://doi.org/10.1063/1.3525931

[21] J.-H. Lee, C. Park, K.-S. Im, and J.-H. Lee, “AlGaN/GaN-based lateral-type schottky barrier diode with very low reverse recovery charge at high temperature,” *IEEE Trans. Electron Devices.*, vol. 60, no. 10, pp. 3032–3039, Oct. 2013, doi: 10.1109/TED.2013.2273271.

[22] X. Li, T. Pu, L. Li, and J.-P. Ao, “Enhanced sensitivity of GaN-based temperature sensor by using the series schottky barrier diode structure,” *IEEE Electron Device Lett.*, vol. 41, no. 4, pp. 601–604, Apr. 2020, doi: 10.1109/LED.2020.2971263.

[23] L. Li *et al.*, “GaN Schottky Barrier Diode with TiN Electrode for Microwave Rectification,” *IEEE J. Electron Devices Soc.*, vol. 2, no. 6, pp. 168–173, Nov. 2014, doi: 10.1109/JEDS.2014.2346395.

[24] M. Trivedi and K. Shenai, “Performance evaluation of high-power wide band-gap semiconductor rectifiers,” *J. Appl. Phys.*, vol. 85, pp. 6889–6897, Apr. 1999. [Online]. Available: http://doi.org/10.1063/1.370208